

Interfacial reactions and mechanical properties of W–SiC in-situ joints for plasma facing components

S.J. Son ^{a,c,*}, K.H. Park ^a, Y. Katoh ^b, A. Kohyama ^c

^a Graduate School of Energy Science, Kyoto University, Gokasho Uji, Kyoto 611-0011, Japan

^b Oak Ridge National Laboratory, Oak Ridge, TN 37831-6138, USA

^c Kohyama Laboratory, Institute of Advanced Energy, Kyoto University, Gokasho Uji, Kyoto 611-0011, Japan

Abstract

Joints of tungsten and SiC were produced by a hot-pressing method and characterized on interfacial reaction and ambient temperature mechanical properties. Reaction phases were identified and the diffusion path was demonstrated by means of quantitative analysis. Four distinctive reaction phases, namely tungsten silicides (WSi_2 , W_5Si_3) and tungsten carbides (WC , W_2C), were formed in various processing conditions. Complex reactions were confirmed in tungsten–SiC diffusion pair, and the diffusion path was experimentally verified as $SiC/WSi_2/WC/W_5Si_3/W_2C/W$. Mechanical properties of the joints were evaluated by flexural and shear tests. Joint shear strength as high as ~ 90 MPa was obtained even when substantial interfacial reaction occurred, however, excessive growth of the reaction layer caused a severe degradation in strength.

© 2004 Elsevier B.V. All rights reserved.

1. Introduction

Silicon carbide (SiC) and SiC fiber-reinforced SiC matrix composites (SiC/SiC composites) are considered as attractive structural materials for fusion reactors, because of their excellent physical, chemical and nuclear properties under anticipated fusion environments. For the application of these materials to gas-cooled fusion blanket systems, they have to satisfy specific requirements, such as hermeticity and surface features, in addition to baseline thermo-mechanical and irradiation properties. The remaining critical issues include those associated with joining, heat transfer and plasma-surface interactions [1–5]. Tungsten as a coating material for SiC-based plasma-facing components has excellent advantages, such as a small mismatch in coefficient of thermal expansion (CTE), a very low sputtering yield,

inherent heat resistance and high thermal conductivity [6,7].

Objective of this series of work is to help designing and developing time- and cost-efficient processes to fabricate tungsten-coated SiC and SiC/SiC composites. As the first step, scoping of solid state bonding between SiC and tungsten during hot-pressing was performed, where the bonding mechanisms and the chemical reactions have been inspected [8,9]. Based on the results, in-situ and sequential tungsten coatings on SiC/SiC composites have been investigated.

In the present work, micron-sized tungsten and nano-phase SiC powders were hot-pressed simultaneously and sequentially, in order to systematically prepare test samples. Various reaction processes in the tungsten–SiC system were quantitatively studied by microstructural and microchemical analyses for the identification of optimized fabrication process.

2. Experimental procedure

Nano-phase SiC powder (particle size < 30 nm, purity $> 95\%$) and tungsten powder (average particle

* Corresponding author. Address: Kohyama Laboratory, Institute of Advanced Energy, Kyoto University, Gokasho Uji, Kyoto 611-0011, Japan. Tel.: +81-774 38 3465; fax: +81-774 38 3467.

E-mail address: sjson@iae.kyoto-u.ac.jp (S.J. Son).

size: 0.6 μm , 99.9% purity) were used as the starting materials. The amount of powder for single batch was controlled to obtain the same thickness for tungsten and SiC layers. The process conditions were selected so that sufficiently sintered SiC with Al_2O_3 based sintering additives could be obtained. Specifically, for the tungsten-SiC ‘in-situ’ joining, the hot-pressing temperatures, pressure and hold-time were 1700–1900 $^\circ\text{C}$, 20 MPa and 10–120 min, respectively. The fabricated samples were machined by a diamond cutting wheel and polished for mechanical property test and microstructural observation.

For the characterization, reaction layers created at the interface between tungsten and SiC were quantitatively analysed on microstructural and microchemical aspects. Phase identification was performed by using a X-ray diffractometer and an energy dispersive X-ray spectrometer attached to the field emission-scanning electron microscope (FE-SEM) (JSM-6700F, JEOL) [10–13]. Mechanical properties were evaluated by three-point flexural test and shear test using an electro-mechanical test frame (Model 5581, Instron, Inc.). The three-point flexural test with specimen size of $22(l) \times 2(w) \times 2(t)$ mm^3 was performed with the support span of 18 mm and the crosshead speed of 0.5 mm/min (W on tension side). Shear strength test was conducted with the specimen geometry of $3(l) \times 3(w) \times 2(t)$ mm^3 and the specimen setting for the test was arranged to make the peak of stress concentration within the reaction layers [14–16]. The fracture surfaces were observed using an FE-SEM.

3. Results and discussion

As the tungsten-SiC joint specimens were produced through a simultaneous pressure-sintering of tungsten and SiC, interphases of substantial thickness were present as the result of reaction in all the process conditions. Fig. 1(a)–(c) show fracture surfaces, including the reaction products, of the flexural-tested samples were fabricated at different temperatures. Thickness of the

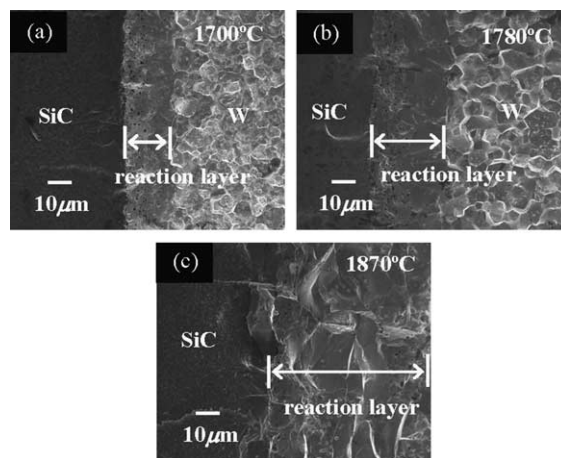


Fig. 1. Fracture surface of the flexural-tested W-SiC joints processed at (a) 1700 $^\circ\text{C}$, 20 MPa, (b) 1780 $^\circ\text{C}$, 20 MPa, and (c) 1870 $^\circ\text{C}$, 20 MPa.

reaction layer increased with the increasing process temperature, as well as the appearance of the reaction layer and grain size of the sintered tungsten showed distinct dependence on it.

The result of reaction phase identification is summarized in Table 1. Four reaction phases, namely WSi_2 , WC , W_5Si_3 and W_2C , were identified. At temperatures below 1750 $^\circ\text{C}$, the production of WSi_2 and WC phases was preferred. WSi_2 did not appear at the higher process temperatures, while WC gradually reduced its amount with as temperature increased. W_5Si_3 , which was produced at temperature of 1780 $^\circ\text{C}$ or above, and W_2C became the stable and dominant phases at high temperatures (see Table 1(a)). The result of time evolution study in Table 1(b) confirmed the preferred stability of W_5Si_3 and W_2C at 1780 $^\circ\text{C}$.

WSi_2 and WC phases as the initially produced reaction phases were then transformed into the stable W_5Si_3 and W_2C phases with the increase of process temperature and duration. Amount and fractional phase distribution of the reaction products will thus be controllable

Table 1

Summary of the phase identification result: (a) at 60 min of process time; (b) at 1780 $^\circ\text{C}$ of process temperature

(a) Process temperature ($^\circ\text{C}$)	1700	1750	1780	1800	1850	1870	1900
Created reaction phases	W_2C	W_2C	W_2C W_5Si_3	W_2C W_5Si_3	W_2C W_5Si_3	W_2C W_5Si_3	W_2C W_5Si_3
	WC	WC	WC	WC	WC	WC	WC
	WSi_2	WSi_2					
(b) Process time (min)	10	30	60	90	120		
Created reaction phases	W_2C	W_2C	W_2C W_5Si_3	W_2C W_5Si_3	W_2C W_5Si_3		
	WC	WC	WC	WC			

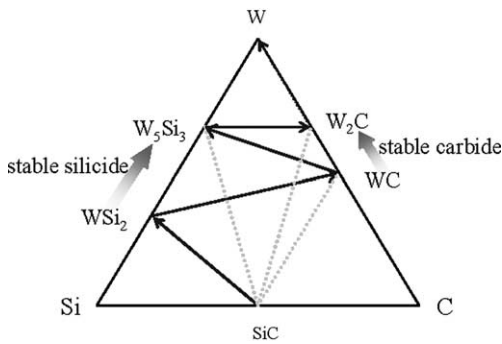


Fig. 2. Representative schematic of the proposed diffusion path at the W–SiC interface during the elevated temperature reaction.

by selecting an appropriate condition of processing. A schematic illustration of diffusion path from the phase analysis is presented in Fig. 2.

Elemental composition across the reaction layer was line-profiled by EDS, as shown in Fig. 3, on the fracture surface of flexural-tested specimen processed at 1780 °C. The XRD results were used for validation of phase identification. As obvious in the compositional profile, the reaction layer appeared to comprise of distinctive layers of the mixture of reaction product phases. The

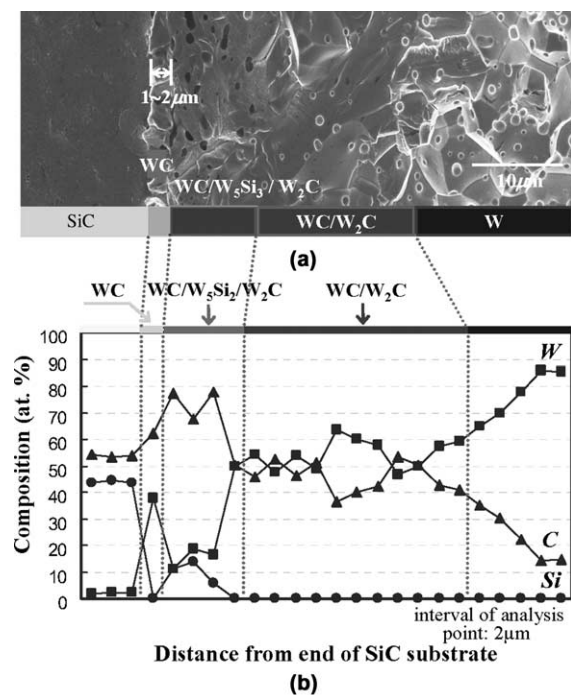


Fig. 3. (a) Fracture surface and (b) compositional line profiles across the reaction layer in the flexural-tested W–SiC joint produced at 1780 °C for 60 min.

same or very similar patterns were confirmed for other process conditions.

Fig. 4 shows the influences of process temperature and time on the flexural strength and the reaction layer thickness. In Fig. 4(a), flexural strength exhibited its maximum at temperature of 1780–1800 °C, at which the reaction layer thickness was about 33 μm. The processing at the temperature above 1870 °C caused a rapid increase in thickness, which was accompanied with the serious deterioration of strength. In Fig. 4(b), the flexural strength shows its maximum at the layer thickness of about 40 μm. It is likely that the flexural strength increased with the more complete sintering of SiC and tungsten was achieved as the temperature and process time increased, until thickness of the reaction layer reached a critical value of ~50 μm for the severe strength deterioration.

In Fig. 5(a) and (b), the result of shear strength evaluation and examples of the shear fracture surfaces are presented. The fracture seemed to have originated at or close to the interface between reaction layer and SiC substrate, and then the crack seems to have propagated within the reaction layer until the total rupture. The higher shear strength of W–SiC joints produced at 1780 °C compared to those produced at 1800 °C confirms the detrimental effect of reaction layer thickness on the joint strength. However, the absolute shear strength

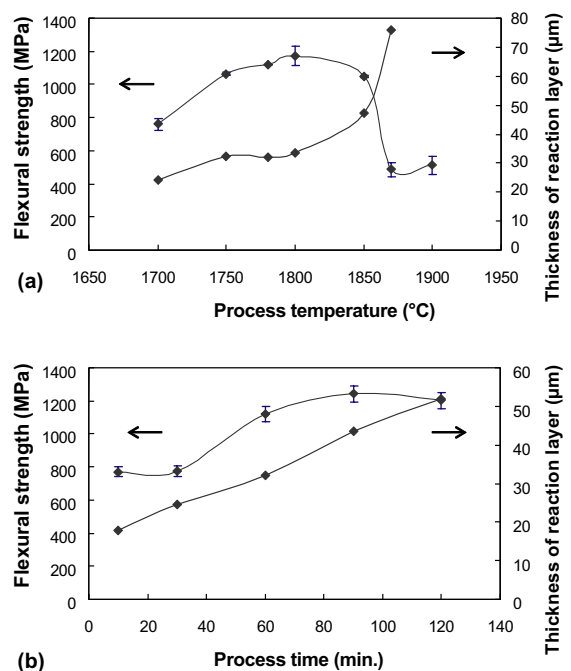


Fig. 4. The influences of processing condition on flexural strength and the total thickness of reaction layers; (a) at 60 min of process time, and (b) at 1780 °C of process temperature.

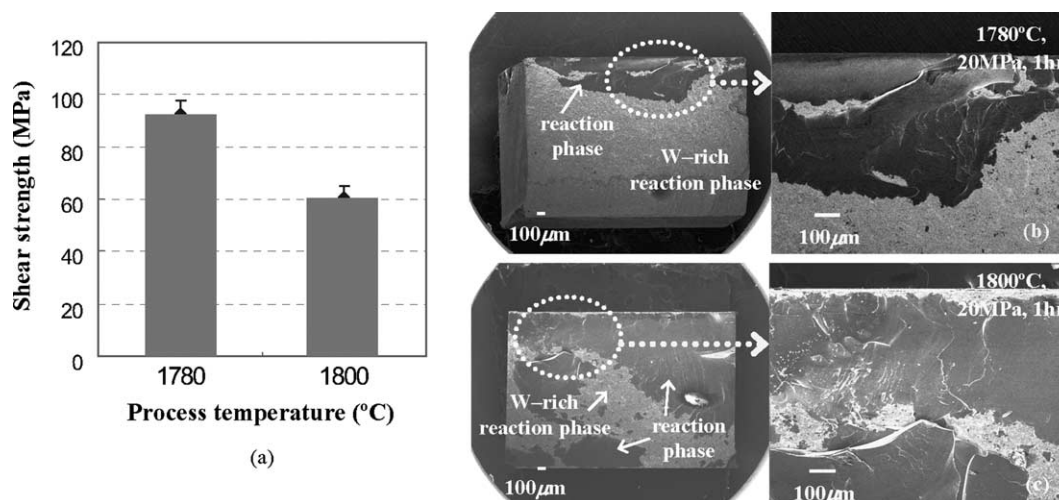


Fig. 5. Measured shear strength and the fracture surfaces of W–SiC joints.

of ~90 MPa obtained for the 1780 °C-produced joints is very high for the tungsten–SiC joint systems.

4. Conclusion

Solid state reaction of hot-pressed W–SiC in-situ joints was investigated. The reaction products were analysed for phase and amount in a range of processing temperature and time. The reactions at interfaces led to diffusion path along SiC/W₅Si₃/WC/W₂C/W in many cases.

The fabricability of W–SiC joints with reliable bonding strength was demonstrated using a hot-pressing method. The applicability of this in-situ joining and the derivative coating/joining techniques to plasma facing components needs to be further studied in many aspects including mechanical integrity, thermal stability, fatigue life time and irradiation effects.

References

- [1] R.H. Jones, L.L. Snead, A. Kohyama, P. Fenici, *Fus. Eng. Des.* 41 (1998) 15.
- [2] Y. Hirohata, T. Jinushi, Y. Yamauchi, M. Hashiba, T. Hino, Y. Katoh, A. Kohyama, *Fus. Eng. Des.* 61&62 (2002) 699.
- [3] R.H. Jones, L. Ciancarli, A. Hasegawa, Y. Katoh, A. Kohyama, B. Riccardi, L.L. Snead, W.J. Weber, *J. Nucl. Mater.* 307–311 (2002) 1057.
- [4] C.A. Lewinsohn, M. Singh, T. Shibayama, T. Hinoki, M. Ando, Y. Katoh, A. Kohyama, *J. Nucl. Mater.* 283–287 (2000) 1258.
- [5] A. Hasegawa, A. Kohyama, R.H. Jones, L.L. Snead, B. Riccardi, P. Fenici, *J. Nucl. Mater.* 283–287 (2000) 128.
- [6] Y. Ueda, K. Tobita, Y. Katoh, *J. Nucl. Mater.* 313–316 (2003) 32.
- [7] A. Kurumada, Y. Imamura, Y. Tomota, T. Oku, Y. Kubota, N. Noda, *J. Nucl. Mater.* 313–316 (2003) 245.
- [8] W.F. Seng, P.A. Barnes, *Mater. Sci. Eng. B* 72 (2000) 13.
- [9] F. Goesmann, R.S. Fetzner, *Mater. Sci. Eng. B* 46 (1997) 357.
- [10] L. Baud, C. Jaussaud, R. Madar, C. Bernard, J.S. Chen, M.A. Nicolet, *Mater. Sci. Eng. B* 29 (1995) 126.
- [11] F. Goesmann, R.S. Fetzner, *Mater. Sci. Eng. B* 34 (1995) 224.
- [12] Y. Gao, S. Zheng, K. Zhu, *Mater. Lett.* 50 (2001) 358.
- [13] A.E. Martinelli, R.A.L. Drew, *Mater. Sci. Eng. A* 191 (1995) 239.
- [14] P. Colombo, B. Riccardi, A. Donato, G. Scarinci, *J. Nucl. Mater.* 278 (2000) 127.
- [15] C.A. Lewinsohn, R.H. Jones, P. Colombo, B. Riccardi, *J. Nucl. Mater.* 307–311 (2002) 1232.
- [16] A.E. Martinelli, R.A.L. Drew, *J. Eur. Ceram. Soc.* 19 (1999) 2173.